Design considerations of an electromechanical generator implanted in human total knee prosthesis

Gabriele Baronio*

Department of Mechanical and Industrial Engineering,
University of Brescia,
Branze 38, 25123 Brescia, Italy
E-mail: gabriele.baronio@ing.unibs.it
*Corresponding author

Vincenzo Luciano, Emilio Sardini and Mauro Serpelloni

Department of Information Engineering,
University of Brescia,
Branze 38, 25123 Brescia, Italy
E-mail: vincenzo.luciano@ing.unibs.it
E-mail: emilio.sardini@ing.unibs.it
E-mail: mauro.serpelloni@ing.unibs.it

Abstract: The energy generation inside the human body represents a crucial aspect for powering implantable measuring circuits. In this work, a system for the electromagnetic energy harvesting, implantable in a total knee prosthesis (TKP) and capable of generating electricity from the knee movement, is presented. The energy harvesting system (EHS) is composed of two series of NdFeB magnets, located on each condyle, and a coil placed in a pivot of the tibial tray. The operating principles, design considerations and performed simulations are shown. Simulation results demonstrate that it is possible to generate an alternating voltage of maximum 600 mV. The proposed generator eliminates the batteries inside the human body and the use of techniques for the inductive power supply. The structural changes with respect to commercial prosthesis are minimal. Furthermore, the proposed energy harvester allows to generate electricity without changing or hindering the patient natural movement.

Keywords: total knee prosthesis; TKP; electromechanical generator; human energy harvesting.

Reference to this paper should be made as follows: Baronio, G., Luciano, V., Sardini, E. and Serpelloni, M. (2013) 'Design considerations of an electromechanical generator implanted in human total knee prosthesis', *Int. J. Mechatronics and Manufacturing Systems*, Vol. 6, No. 3, pp.270–284.

Biographical notes: Gabriele Baronio is an Assistant Professor of Engineering Design in the Department of Mechanical and Industrial Engineering at the University of Brescia. He teaches in technical drawing and computer-aided design. Currently, the research activity is mainly focused on design and development of biomedical devices and aids for the disabled people.

Vincenzo Luciano is a PhD student in Mechatronics at the University of Bergamo in the Department of Information Engineering at the University of Brescia. Currently, his research activity is mainly focused on design and development of energy harvesting systems for biomedical devices.

Emilio Sardini graduated in 1983 in Electronic Engineering from the Polytechnic of Milan. Since 1984 he conducts research and teaching activities at the Department of Electronics for Automation, University of Brescia. Since January 11, 2006 he is a Full Professor of Electrical and Electronic Measurement. He has been a member of the Integrated Academic Senate and of the Board of Directors of the University of Brescia. Now he is the Coordinator of the 'Technology for Health' PhD programme, member of the College of Mechatronics PhD at the University of Bergamo and Director of Department of Information Engineering. He has done intensive research in the field of electronic instrumentation, sensors, and signal conditioning electronics. Recently, his research has been addressed to the development of autonomous sensors for biomedical applications. He is author or coauthor of more than 100 papers published in international journals or proceedings of international conferences.

Mauro Serpelloni is currently an Assistant Professor of Electrical and Electronic Measurements with the Department of Information Engineering, University of Brescia. He has worked on several projects relating to the design, modelling, and fabrication of measurement systems for industrial applications. His research interests include contactless transmissions between sensors and electronics, contactless activation for resonant sensors, and signal processing for micro-electromechanical systems.

This paper is a revised and expanded version of a paper entitled 'Electromechanical generator implanted in a human total knee prosthesis' presented at 1st International Conference on Design and PROcesses for MEdical Devices (PROMED), Brescia, Italy, 2–4 May 2012.

1 Introduction

The current lifetime of about 90% of total knee prosthesis (TKP) is limited at 10 to 15 years (Austin et al., 2004). The revision of a primary TKP is, then, a highly probable event. The study of the problems of the prosthesis and their possible solutions require a more correct design of the prosthetic geometries (Currier et al., 2005). Therefore, the possibility of knowing different parameters in-vivo, e.g., the force distributions on the articular surfaces, allows to use these information for a more deep analysis of the prosthetic implant. The technique that ensures a good knowledge of the loads, and then a better analysis of prosthetic implants, is based on an in-vivo real-time monitoring of the articular surface stress conditions (Almouahed et al., 2008; Kondo et al., 2008). In the literature, sensorised prostheses able to measure in-vivo the contact forces and to wirelessly transmit these ones outside the human body are proposed (D'Lima et al., 2005, 2007). In D'Lima et al. (2007), the results show an acceptable accuracy in knowledge of the loads acting on the tibial plate.

The principal difficulty in in-vivo measurement is that the implanted system has to be autonomous. Therefore, the necessary energy for the functioning cannot be provided by

batteries, which require periodic substitutions, or by cabled solutions between the inside and the outside of the human body. All the previous cited works (D'Lima et al., 2005, 2007) use an external coil winded to the knee, and properly supplied, which has the double function of powering and transferring the data between the implanted device and the external readout unit. This solution, though it provides from the outside the power-supply, adds a complication to the patient that has to wear a band and limits the possibilities of using the system in all the situations. Then an integrated energy harvester implanted inside the human body could be a viable solution for feeding an implantable measuring circuit with the aim to measure different parameters in-vivo for the whole lifetime.

Different studies are proposed to harvest energy from human movements, particularly for electronic devices (Mitcheson et al., 2008). In Turri and Benbouzid, (2009), a device that exploits the knee movement using an oscillating device is presented. The device is optimised to be implanted in the prosthesis and preliminary results show a total power output of about 850 μW. In Almouahed et al. (2011), a different principle of conversion is proposed obtaining, at the same time, a measurement of the forces acting on the tibial tray and the energy generation for the electronic measurement system functioning.

In the present work, analysis and design considerations of a proposed electromechanical generator implanted in human TKP are presented. The generator harvests the mechanical energy related to knee motion and converts it into electric energy. The proposed device is based on a direct conversion of the relative motion of tibia and femur, without motion or deformation of any other object, as commonly happens in other piezoelectric, inertial [electromagnetic or electrostatic (Baginsky et al., 2010)] or fluidic (Wang and Chang, 2010) energy harvesting systems (EHSs). This aspect allows the proposed EHS integration with less variation in the stiffness and reduced technical complications than the previous aforesaid EHSs.

In fact, the alterations carried out on the original implant are little invasive and the prosthesis mechanical behaviour is guaranteed leaving almost unaltered the structural weak parts. In particular, the modifications on the titanium femoral component do not change the prosthesis stiffness, and the modifications on the polyethylene tibial tray are limited to the pin which is not subjected to high level of stress.

In the following sections, the device electromechanical aspects are discussed, and, subsequently, proposed generator simulations were implemented in order to obtain design considerations for the generator. The discussion that follows shows the issues and design decisions that have been taken in accordance with the project goals and the results reported.

2 Electromechanical working principle and description of the CAD model

2.1 Electromechanical working principle

The TKP consists of two parts: the femoral component (condyles) and the tibial components (articular insert + tibial plate). Figure 1(a) shows the TKP components. The proposed EHS is totally integrated in these components; it is composed of two series of NdFeB magnets, located on each condyle, and a coil placed in the pivot of the tibial tray. During the human body movement (walking) a relative motion between the tibial and femoral components of TKP occurs. During this movement, through the magnets in the

femoral component (condyles) and the coil in the articular insert, an electromotive force is generated according with the Faraday-Neumann-Lenz's law. This electromotive force can be used to power up a measurement system that can be housed in the articular insert. Figure 1(b) shows a prosthesis section in the sagittal plane in which the magnets and coil are shown.

Figure 1 (a) ZIMMER NexGen® Legacy® Knee LPS-Flex prosthesis, (b) Prototype section-view: condyle with magnets and relative housings, and articular insert with coil and the future force sensor system housing (see online version for colours)

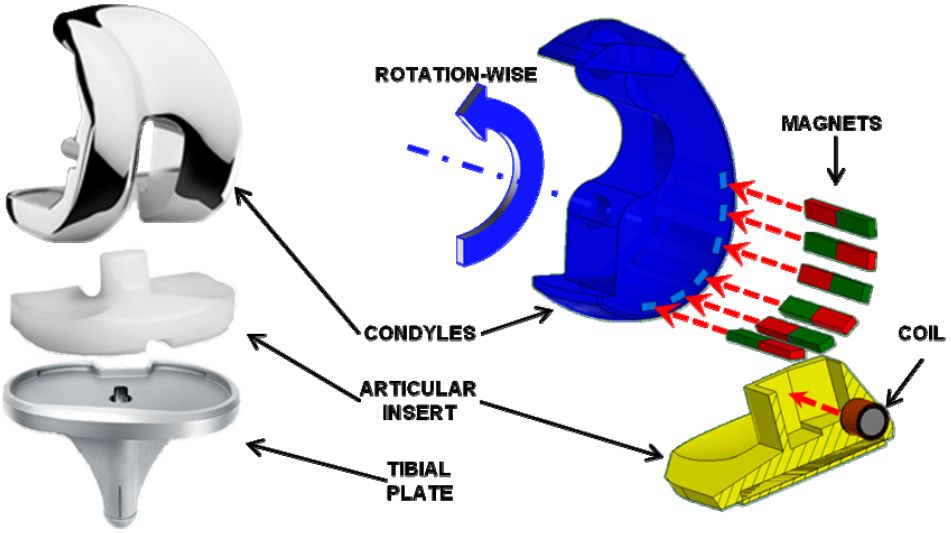

(a) (b)

As already described in Luciano et al. (2012), the prosthesis was designed with a CAD tool starting from the reverse engineering of an actual prosthesis (Figure 2). Subsequently, some modifications were developed in order to house the new items: magnets and coil [Figure 1(b)].

Figure 2 A stage of the prosthesis reverse engineering

Six magnets were inserted in six prismatic housings, placed in the thickness of each condyle with the magnetic axis parallel to the articular insert surface.

The six magnet housings outline two arcs of circumference (three magnets each). One arc is concentrical to the red circumference (Figure 3). One arc is concentrical to the blue circumference (Figure 3). The two circumferences (red and blue) define the actual prosthesis condyle profile.

Figure 3 Housing of magnets (see online version for colours)

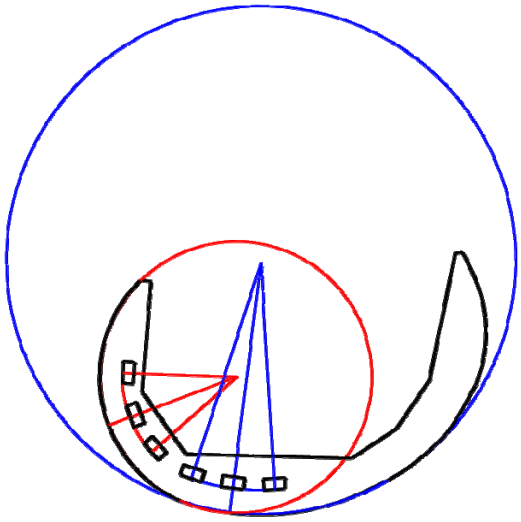

Between the two condyles, a cavity is realised in the tibial plate prominence, in which the copper coil can be inserted with its axis parallel to the magnet magnetic axis (green hatch in Figure 4).

Figure 4 Coil housing in the tibial plate prominence (see online version for colours)

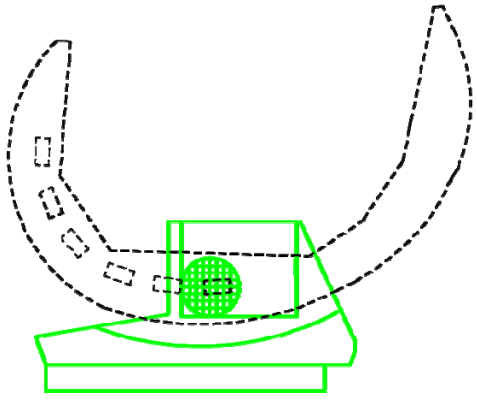

This way, the relative motion between femur and tibia induces a potential difference on the coil according to Faraday-Neumann-Lenz's law.

Two magnets in the condyles, aligned on the same line, have the same magnetic axis orientation, while two following magnets, on each condyle, have opposite magnetic axis. The reason is to obtain a more rapid variation of the magnetic field induced on the coil and a resulting higher induced voltage. Furthermore, core in permalloy is inserted in the coil with the aim of improve the flux linkage.

2.2 CAD model description

In the present paragraph, the relative movement between the tibial and femoral components was studied by use of a CAD tool in order to outline a synthesised mechanical system.

This synthesised mechanical system allows to achieve two goals: firstly, the system permits to reproduce the movement steps necessary for electromechanical FEM simulations. Secondly, the system permits to design a test prototype (to be built by use of 3D printer technology).

The relative motion between the tibial and femoral components with respect to the sagittal plane is a rototranslation. The movement projection on the sagittal plane was studied by use of a CAD tool.

The system was synthesised as a crank-rocker mechanism (Figure 5): the crank (OA) is connected to the motor, the rod (AB) represents the femoral component, the rod (BO^1) is the rocker arm and the segment (OO^1) is the fixed frame.

The difference in length between the crank (OA) and the rocker arm (O^1B) generates a femoral component motion (AB) characterised by an instant centre of rotation influenced by the position of points O^1 (in the first part of rototranslation) and O (in the second part of rototranslation).

The quadrilateral is designed to reproduce the prosthesis motion in the first 60° of tibia-femur rotation (Figure 6). This angle portion is useful for the power production during activity (McClelland et al., 2011).

This three-dimensional model was used to determine the geometrical position of magnets and coil along the 60° angle of the prosthesis actual rototranslation. The angle was divided in thirteen steps of 5° each.

Figure 5 The mechanism $OABO^1$ view that moves the condyles containing the magnets with respect to the articular insert containing coil P (see online version for colours)

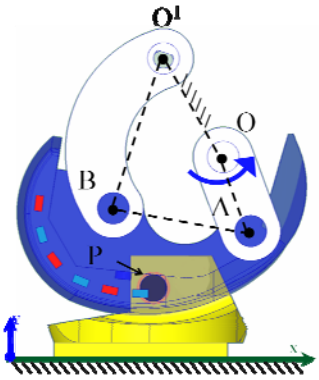

Figure 6 Angle of tibia-femur rotation (see online version for colours)

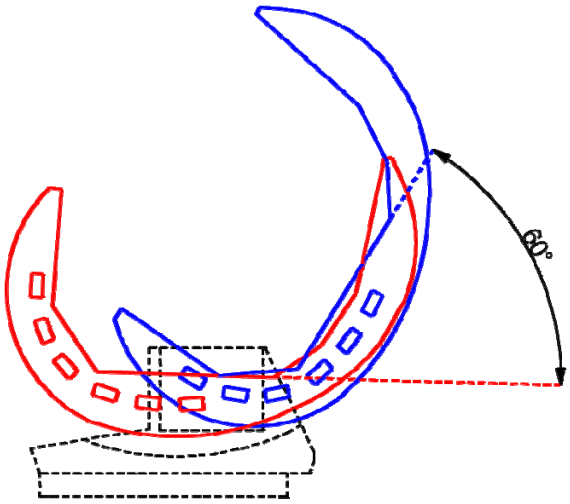

3 Electromechanical fem simulations

In order to obtain a first indication of the conceived system functioning, a numerical evaluation of the electromotive force generated by it was implemented. As reported in Section 2, the geometric and kinematic parameters, which describe the system physical model, were fixed. The remaining parameters necessary for a finite element simulation analysis of the induced electromotive force are the physical and geometric characteristics of the magnets, coil and its core.

The commercial software products for finite-element electromagnetic simulations are able to simulate only a purely rotational or translational motion. So in this case, in which the magnets move off respect to the coil with a composed motion, an alternative solution was followed. For recreating a situation, as more as possible corresponding to the real one, the motion imposed by the designed kinematic chain was subdivided in a discrete sequence of configurations. In particular thirteen step-configurations were considered every five degrees from the complete rotation from 0° to 60°. In each step-configuration, a magnetostatic analysis was performed, and the electromagnetic induction on each coil was carried out. In this analysis, the magnet relative position with respect to themselves and with respect to the coil was considered an important aspect for the EHS.

With the aim to define the design strategies, the analyses of three possible configurations were considered.

The first simulation (Figure 7) uses the coil placed in a position chosen to fit the magnet trajectories. The magnets are oriented concentrically to the two condyle circumferences.

Figure 7 First configuration (see online version for colours)

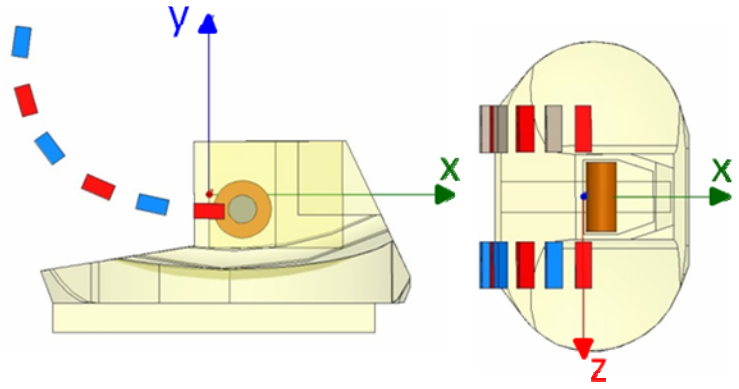

The second case, Figure 8, considers the same coil of the previous one, but subdivided in two halves symmetrically placed with respect to the sagittal plane (xy). This configuration permits to reduce the space occupied by the coil in the tibial pin. The electromotive force is the sum of the two contributions.

Figure 8 Second configuration (see online version for colours)

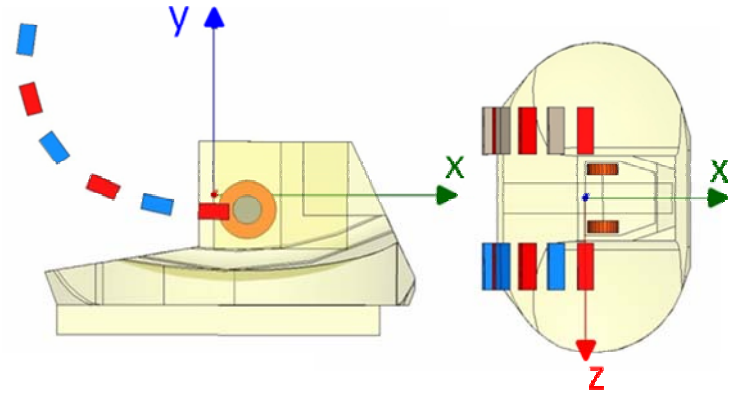

Figure 9 Third configuration (see online version for colours)

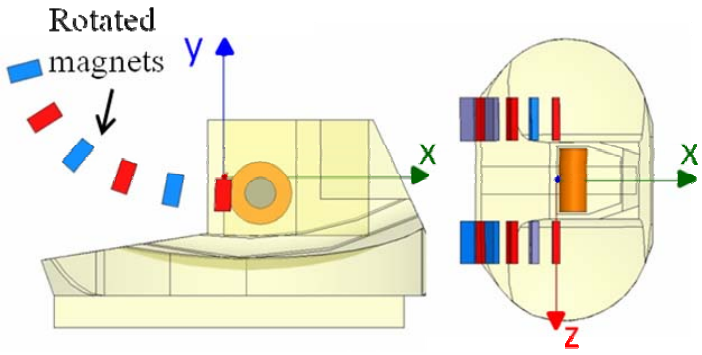

The last simulation considers a different magnet disposition; they are rotated about the magnetic axis of 90° (Figure 9). In this configuration, the magnetic flux coupled with the coil is different due to the rotated magnetic axis. Furthermore, the consecutive magnets are more distant from each other, therefore less influenced each other.

The physical and geometric data of the magnets, core-coil and coil used in the three simulations are chosen referring to available commercial products and reported in the following Tables 1 and 2.

Table 1 Physical data of the coil, ferrite and magnets

Element	*Parameters [unit]*	*Value*
Coil	Material wire	copper
	diameter wire [mm]	0.2
Core-coil	Material	Permalloy
	Relative permeability [1]	150000
	Electrical resistivity[mohm/cm]	59
Magnets	Material	Neodymium N45 (NdFeB)
	Residual induction [mT]	1320-1380
	Coercive force [kAm^{-1}]	923
	Intrinsic coercive force [kAm^{-1}]	955
	Energy product BH_{MAX} [kJm^{-3}]	342–366
	Max operating temperature [°C]	80

Table 2 Geometrical data of the magnets, coils and coil-core

Case	*Component*	*Dimensions [mm]*
1-2-3	Magnets	
	(length-height-width)	(4-2-3)
	mean pitch	4
1	Coil P	(7.8–17.9)
	Core-coil P	(3.8–17.9)
	(diameter-length)	
2	Coil P1, Coil P2	(17.9–3.0)
	Core-coils P1	(3.8–3.0)
	(diameter-length)	
3	Coil P_2 × 4_4	(7.8–17.9)
	Core-coil	(3.8–17.9)
	(diameter-length)	

The method used to calculate the total induced flux in the coil followed the subsequent reasoning. Indicating with

- $n(z)$ [(m^{-1})], the winding distribution per unit of length
- $A(z)$ [(m^2)], the coil cross section (in this case, it is constant)
- l [(m)], the coil length (i.e., for coil A, $l = [z_1, z_2]$ on *z-axis* in Figure 4)
- $\varphi_{solenoid}(\vartheta)$ [(Wb)], the total flux induced in a single solenoid, in each single angular configuration ϑ,

then, the flux was carried out using expression (1):

$$\varphi_{solenoid}(\vartheta) = \int_{z_1}^{z_2} n(z)dz \iint_{A(z)} \overrightarrow{B(x,y,z;\vartheta)} \cdot \overrightarrow{dA} =$$
$$= n\int_{z_1}^{z_2} dz \iint_{A} B_z(x,y,z;\vartheta)\, dA = \tag{1}$$
$$= n\iiint_{solenoid} B_z(x,y,z;\vartheta) dA dz$$

In this expression, the dot product evaluation was made considering that only B_z component is necessary as it is clear observing the reference axes in Figure 10.

Figure 10 Example of field distribution ($\vartheta = 20°$) (see online version for colours)

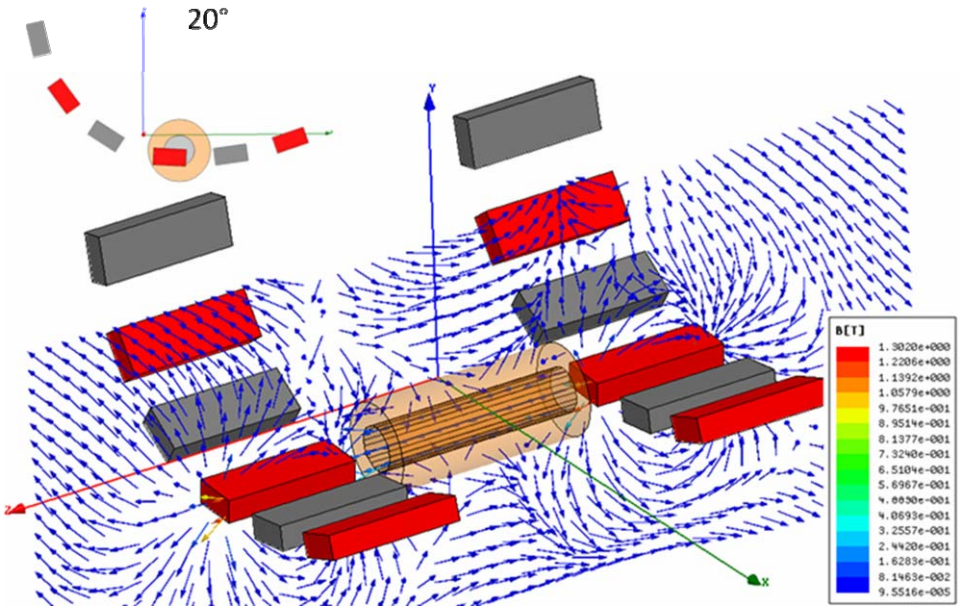

The magnet placement was made trying to maximise the flux variability. The adopted choice is placing two following magnets on the same condyle with opposite magnetic orientation, while two magnets on the two condyles, aligned about z axis, have the same magnetic orientation.

Starting with simulation of case 1 (Figure 7), in order to obtaining information by the distribution of magnetic induction field along the coil, the field distribution was analysed for all the configurations. Figure 10 shows the field distribution for configuration $\vartheta = 20°$ in a plane crossing the inductor and parallel to y-z plane.

The induced flux $\varphi_{solenoid}(\vartheta)$ trend during the sixty degrees, for cases 1, 2, 3, is reported in Figure 11, Figure 12 and Figure 13.

Figure 11 Case 1 – induced flux on the coil (see online version for colours)

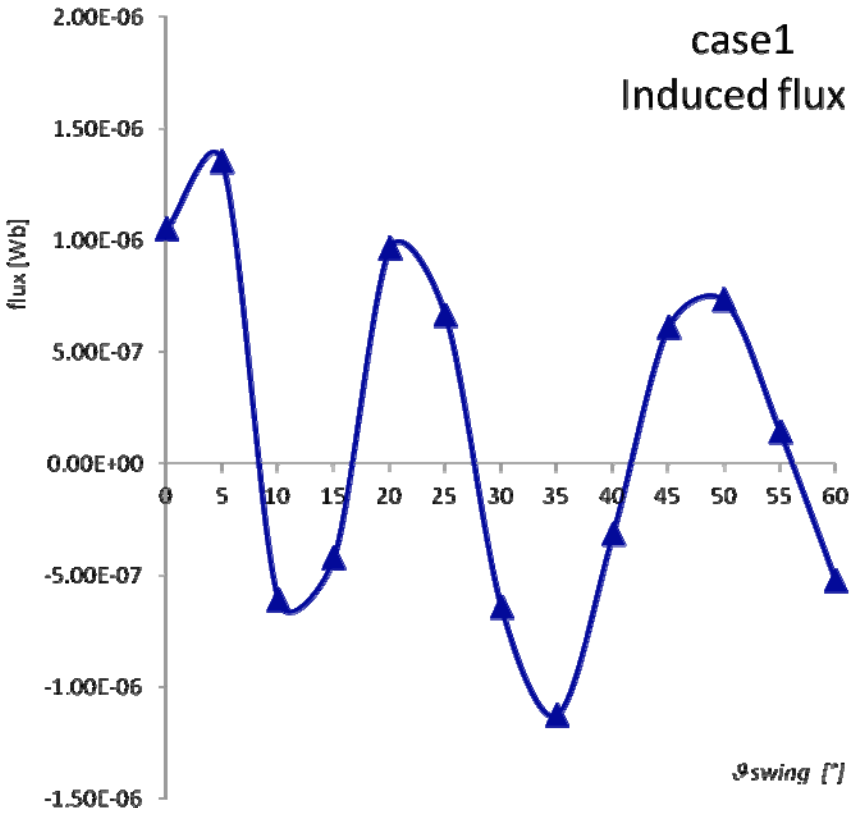

Figure 12 Case 2 – induced flux on the coil (see online version for colours)

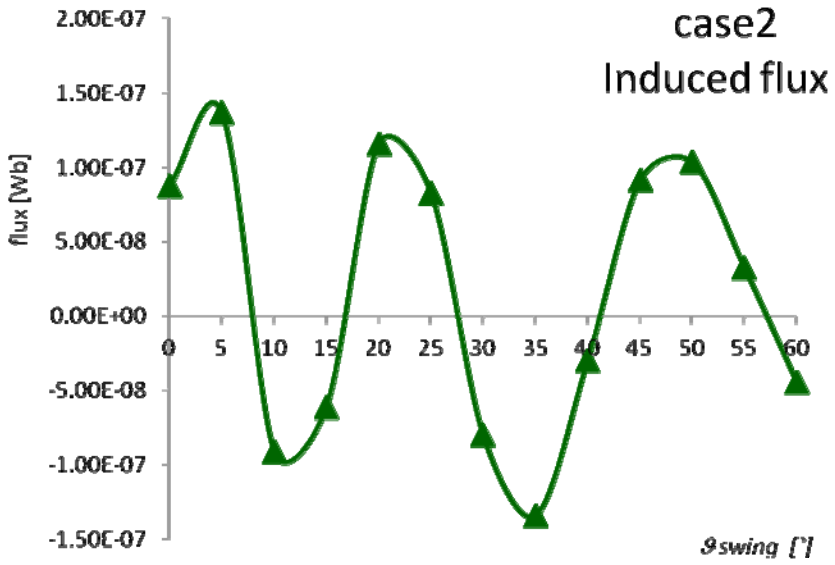

Figure 13 Case 3 – induced flux on the coil (see online version for colours)

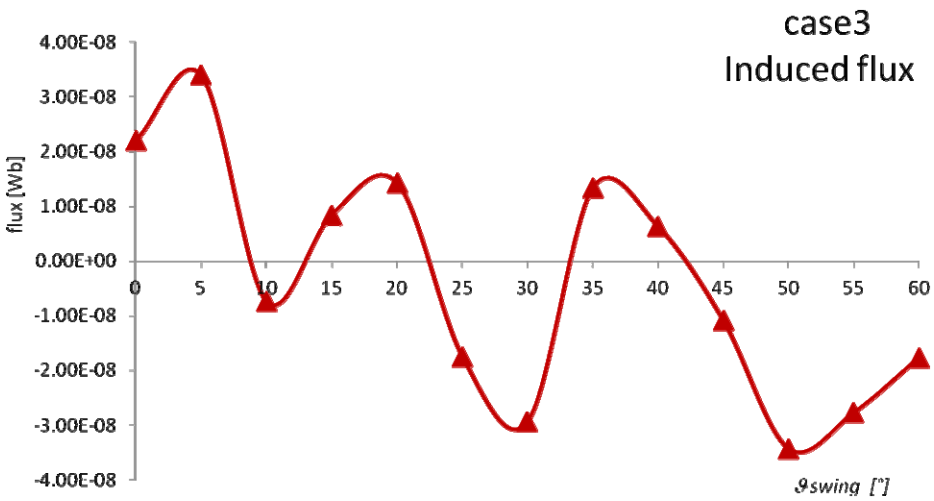

These figures show an alternating flux due to the adopted choice for the magnet placement. The trend is variable from step to step in the sixty degrees for each magnet different trajectory with respect to the coil. The same reason explains the irregularity of the slope in the graphs as well. Analysing the induced flux in cases 1 and 2 it is evident only an amplitude reduction, while in case 3 also a slope reduction is shown.

In fact, in the configuration of case 3 the magnets are rotated, increasing the pitch with respect to the other cases, and the effect is that each magnet induces a flux with lower variability.

The next step is the electromotive force V [(V)] evaluation, expressed by the Faraday-Neumann-Lenz's law.

In order to obtain a relationship of the flux as a function of the time t, it is necessary to know the time variation of the angle ϑ during the considered rotation.

Near to the swing phase, proximately, the rotation of sixty degrees occurs in the 25% of the gait cycle. Assuming that the gait cycle duration is 1.5 s, the average angular velocity $\omega_{avg} = 160°/s$ is calculated (McClelland et al., 2009; Jevsevar et al., 1993).

Using these considerations, the electromagnetic induction law has the following expression:

$$V_i = -\frac{d\varphi_{solenoid}}{dt} = -\frac{d\varphi_{solenoid}}{d\vartheta}\frac{d\vartheta}{dt} = \\ = -\frac{d\varphi_{solenoid}}{d\vartheta}\omega_{avg} \tag{2}$$

where values $\varphi_{solenoid}(\vartheta)$ are provided by the simulation results using equation (1).

In Figure 14, Figure 15 and Figure 16 the graphics of the obtained voltages are shown.

These results show that the first solution (case 1) has the highest peak-to-peak value and lead to the conclusion that for the future prototype analysis the design considerations can consider this configuration as a starting point.

Figure 14 Case 1 – induced voltage on the coil (see online version for colours)

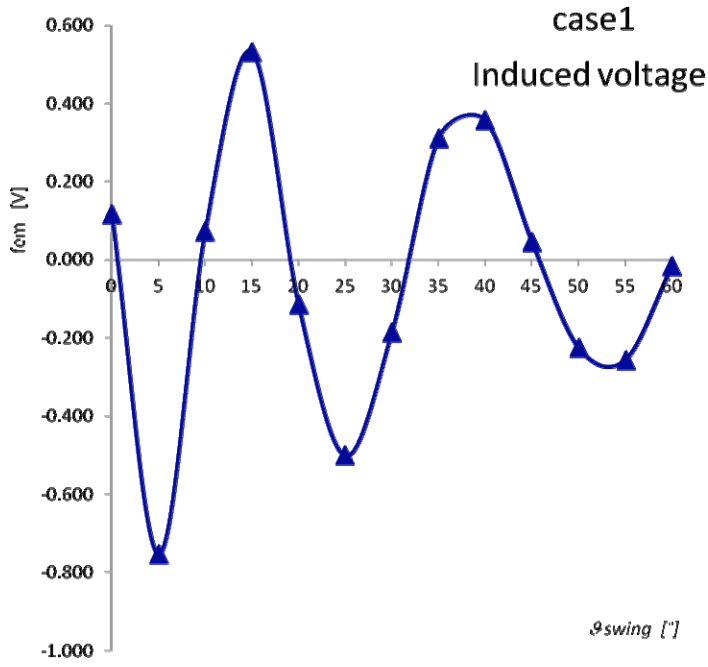

Figure 15 Case 2 – induced voltage on the coil (see online version for colours)

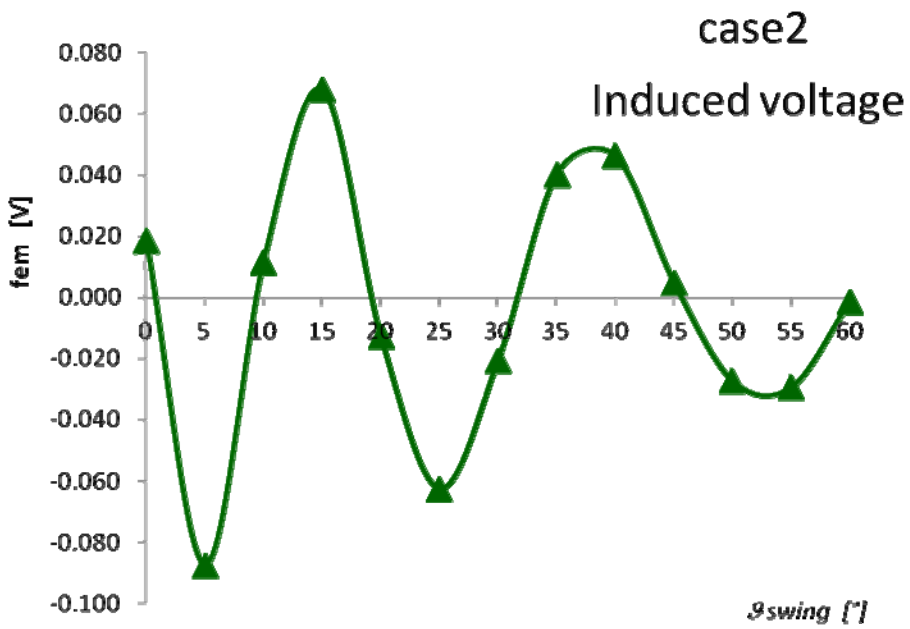

Figure 16 Case 3 – induced voltage on the coil (see online version for colours)

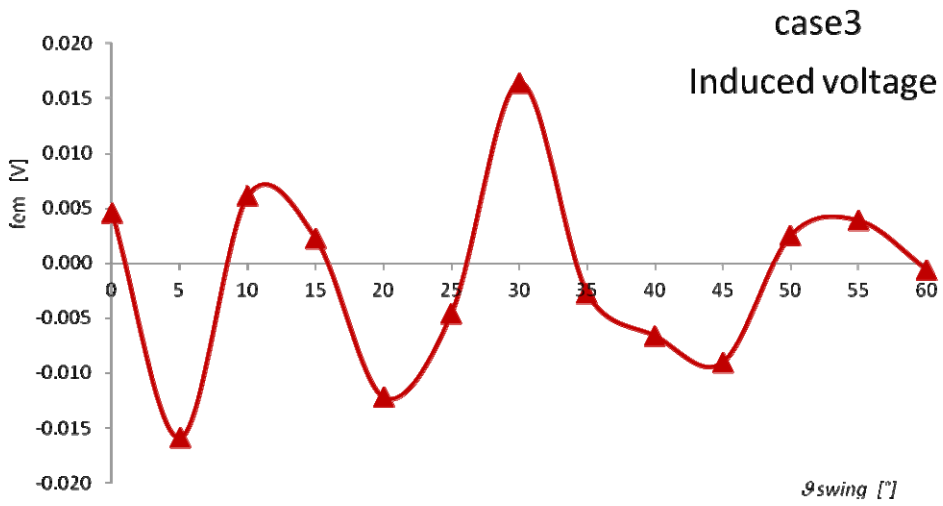

4 Conclusions

The results of simulations and analysis allowed to discuss the power harvesting generator design strategies. The simulation allowed to analyses different configurations of the magnets and coil positions defining the possible configuration that ensures a flow variation in accordance with the objectives. The simulation results allow to affirm that the use of a single inductor, positioned in the insert, and two magnet rows, positioned at the condyle sides, allows to generate an alternating voltage of maximum 600 mV. The discussion on the design considerations revealed that an important aspect of the system is the project simplicity. The changes to be made with respect to a commercial prosthesis are minimal assuring the structure stiffness [the magnet housing realisation in the femoral insert requires a proper technique such as micro drilling (Giorleo et al., 2011) or alternative methodologies (Fiorentino et al., 2012)]. Furthermore, the power harvesting system allows to generate electricity without changing or hindering the patient natural movement. The proposed power harvesting system can be a viable solution for feeding an implantable measuring circuit with the aim to measure different parameters in-vivo for the whole prosthesis lifetime.

References

Almouahed, S., Gouriou, M., Hamitouche, C., Stindel, E. and Roux, C. (2011) 'The use of piezoceramics as electrical energy harvesters within instrumented knee implant during walking', *IEEE/ASME Transactions on Mechatronics*, Vol. 16, No. 5, pp.799–807.

Almouahed, S., Hamitouche, C., Stindel, E. and Roux, C. (2008) 'New trends in instrumented knee prostheses', *Proceeding of 3rd International Conference on Information and Communication Technologies: From Theory to Applications*, pp.1–6.

Austin, M.S., Sharkey, P.F., Hozack, W.J. and Rothman, R.H. (2004) 'Knee failure mechanisms after total knee arthroplasty', *Techniques in Knee Surgery*, Vol. 3, No. 1, pp.55–59.

Baginsky, I., Kostsov, E. and Sokolov, A. (2010) 'Electrostatic microgenerators of energy with a high specific power', *Optoelectronics, Instrumentation and Data Processing*, Vol. 46, No. 6, pp.580–592.

Currier, J.H., Bill, M.A. and Mayor. M.B. (2005) 'Analysis of wear asymmetry in a series of 94 retrieved polyethylene', *Journal of Biomechanics*, Vol. 38, No. 2, pp.367–375.

D'Lima, D.D., Patil, S., Steklov, N., Chien, S. and Colwell, C.W. Jr. (2007) 'In vivo knee moments and shear after total knee arthroplasty', *Journal of Biomechanics*, Vol. 40, Suppl. 1, pp.S11–S17.

D'Lima, D.D., Townsend, C.P., Arms, S.W., Morris, B.A. and Colwell, C.W. Jr. (2005) 'An implantable telemetry device to measure intra-articular tibial forces', *Journal of Biomechanics*, Vol. 38, No. 2, pp.299–304.

Fiorentino, A., Marenda, G.P., Marzi, R., Ceretti, E., Kemmoku, D.T. and Lopes Da Silva, J.V. (2012) 'Rapid prototyping techniques for individualized medical prosthesis manufacturing', *Proceedings of the 5th International Conference on Advanced Research and Rapid Prototyping*, pp.589–594.

Giorleo, L., Ceretti, E. and Giardini, C. (2011) 'ALD coated tools in micro drilling of Ti sheet', *CIRP Annals – Manufacturing Technology*, Vol. 60, No. 1, pp.595–598.

Jevsevar, D.S., Riley, P.O., Hodge, W.A. and Krebs, D.E. (1993) 'Knee kinematics and kinetics during locomotor activities of daily living in subjects with knee arthroplasty and in healthy control subjects', *Physical Therapy*, Vol. 73, No. 4, pp.229–239.

Kondo, M., Fujii, T., Kitagawa, H., Tsumura, H. and Kadoya, Y. (2008) 'Arthroscopy for evaluation of polyethylene wear after total knee arthroplasty', *Journal of Orthopaedic Science*, Vol. 13, No. 5, pp.433–437.

Luciano, V., Sardini, E., Serpelloni, M. and Baronio, G. (2012) 'Analysis of an electromechanical generator implanted in a human total knee prosthesis', *Proceedings of the IEEE Sensors Applications Symposium*, pp.166–170.

McClelland, J.A., Webster, K.E. and Feller, J.A. (2009) 'Variability of walking and other daily activities in patients with total knee replacement', *Gait & Posture*, Vol. 30, No. 3, pp.288–295.

McClelland, J.A., Webster, K.E., Feller, J.A. and Menz, H.B. (2011) 'Knee kinematics during walking at different speeds in people who have undergone total knee replacement', *The Knee*, Vol. 18, No. 3, pp.151–155.

Mitcheson, P.D., Yeatman, E.M., Rao, G.K., Holmes, A.S. and Green, T.C. (2008) 'Energy harvesting from human and machine motion for wireless electronic devices', in *Proceedings of the IEEE*, Vol. 96, No. 9, pp.1457–1486.

Turri, S. and Benbouzid, M.E.H. (2009) 'Preliminary study of a pendulum in vivo electromechanical generator for orthopedic implants', *Proceedings of the IECON: 35th Annual Conference of the IEEE and ICELIE, 3rd IEEE International Conference on E-Learning in Industrial Electronics*, pp.4415–4420.

Wang, D.A. and Chang, K.H. (2010) 'Electromagnetic energy harvesting from flow induced vibration', *Microelectronics Journal*, Vol. 41, No. 6, pp.356–364.